SNRU Journal of Science and Technology

Journal home page: snrujst.snru.ac.th

Microstructural and compositional analyses of segmented $YBa_2Cu_3O_{7-x}$ $NayCoO_2$ oxide thermoelectric ceramic prepared by hot-pressing method

Pimpilai Wannasut[1,2], Poom Prayoonphokkharat[1,2], Nittaya Keawprak[3], Anucha Watcharapasorn[*,1,4]
[1]Department of Physics and Materials Science, Faculty of Science, Chiang Mai University, Chiang Mai, 50200 Thailand
[2]Graduate PhD's Degree Program in Materials Science, Faculty of Science, Chiang Mai University, Chiang Mai, 50200 Thailand
[3]Thailand Institute of Scientific and Technological Research, Pathum Thani, 12120 Thailand
[4]Materials Science Research Center, Faculty of Science, Chiang Mai University, Chiang Mai, 50200 Thailand
[*]**Corresponding Author**: anucha@stanfordalumni.org

Received: 28 December 2017; **Revised**: 10 March 2018; **Accepted**: 28 March 2018; **Available online**: 1 May 2018

Abstract

$YBa_2Cu_3O_{7-x}$-$NayCoO_2$ (YBCO-NCO) oxide thermoelectric ceramic was successfully prepared by hot-pressing method. The optimum procedure included an applied weight of 1 ton, a temperature of 800 °C and 1 h holding time under an Ar atmosphere. The produced segmented bi-layer YBCO-NCO ceramic was highly dense with strong interfacial bonding and well-defined boundary. X-ray diffraction pattern of each layer showed the corresponding phase of each compound. At the interface, chemical bonding between two compounds was expected. This showed that, compared to the conventional sintering method, segmented layers of heterogeneous oxides could be effectively formed using the hot-pressing procedure.

Keywords: segmented oxide thermoelectrics; yttrium barium copper oxide; sodium cobalt oxide

1. Introduction

Nowadays, the growth in various industries has created more demands in electricity and, at the same time, these industrial processes produce waste heat which is currently released to environment without being reused. Thermoelectric conversion is now one of the promising methods to recycle waste heat and, in turn, produce electricity directly for various electronic equipments. Thermoelectric generator is a solid state device which can directly convert heat to electrical energy via Seebeck effect [1, 2]. The performance of a thermoelectric generator is largely determined by the material's characteristics called the dimensionless figure of merit (ZT) expressed by

$$ZT = (\frac{S^2\sigma}{\kappa})\mathrm{T} \quad (1)$$

where S, T, σ and κ are the Seebeck coefficient, absolute temperature, electrical conductivity and thermal conductivity, respectively.

A segmented thermoelectric is one of the composite structures designed to improve the thermoelectric conversion efficiency. Segmented thermoelectric materials were first studied by the Jet Propulsion Laboratory (JPL). They reported that the segmented non-oxide thermoelectric combination of Bi_2Te_3 and $CeFe_4Sb_2$ showed a thermoelectric efficiency over 15% [3]. Furthermore, Ngan *et al.* [4] studied a segmented thermoelectric unicouple made of p-leg $Bi_{0.6}Sb_{1.4}Te_3$-TAGS and n-leg Bi_2Te_3-

PbTe which exhibited the thermoelectric efficiency up to 10%. These results indicated that employing segmented thermoelectric materials according to their temperature dependence of maximum ZT should be viable for high-efficiency thermoelectric devices. Nevertheless, layered or segmented thermoelectrics based on oxide compounds are quite scarce and therefore should be investigated for their high-temperature thermoelectric applications.

Yttrium barium copper oxide ($YBa_2Cu_3O_{7-x}$ or YBCO) is a well-known superconductor with a defect perovskite structure [5]. It has high electrical conductivity (i.e. 50,000 $\Omega^{-1}m^{-1}$ at 300K) [6]. Prayoonphokkharat *et al.* [7] confirmed that $YBa_2Cu_3O_{7-x}$ ceramic had high electrical conductivity (~50,000 $\Omega^{-1}m^{-1}$ at 375K). However, Rodriguez *et al.* [8] reported high electrical conductivity of YBCO to be about $1.0 \times 10^4\ \Omega^{-1}m^{-1}$ Seebeck coefficient of 480 $\mu V\ K^{-1}$ and low thermal conductivity ($\kappa \sim 0.50\ Wm^{-1}K^{-1}$) which resulted in the ZT value ~ 0.30 at 275K. The difference in values of the thermoelectric parameters was likely due to the compositional difference between the YBCO samples prepared under different sintering conditions and the temperature of measurement. Sodium cobalt oxide (Na_yCoO_2 or NCO), where $0.50 \leq y < 1$, has a hexagonal structure. The previous work of Boontham *et al.* [9] found that $Na_{0.6}CoO_2$ had quite high electrical conductivity (77,000 $\Omega^{-1}m^{-1}$ at 300K) and showed ZT value ~0.28 at 675K.

It is well known that the quality of oxide ceramics depends largely on the sintering process. In our previous work [10], attempts to produce the segmented (or bilayer) YBCO-NCO ceramic was successful but the procedure required a rather long processing time which seemed to cause appreciable diffusion of different elemental species across the bilayer boundary. It is also experimentally established that the simultaneously applied pressure and temperature can produce dense ceramic with fine microstructure in a short time period compared to the conventional sintering technique. This was in order to see if the sintering under an applied pressure could allow a better densification rate and, hence, produce a better bi-layered ceramic with strong and uniform interface. The results are discussed in terms of microstructures and compositions across the heterogeneous interface between these two compounds.

2. Materials and Methods

The starting materials for the synthesis of $YBa_2Cu_3O_7$ (YBCO) and $Na_{0.6}CoO_2$ (NCO) powders were Y_2O_3 (99.99%, Aldrich), $BaCO_3$ (≥ 99%, Sigma-Aldrich), CuO (98%, Sigma-Aldrich), Na_2CO_3 (99.50%, Riedel-de Haën) and Co_3O_4 (99.50%, Aldrich). The powders were weighed according to the stoichiometry of each compound, mixed by wet ball milling method for 24 h and dried in an oven. The mixtures for YBCO and NCO were calcined in a normal atmosphere at 850 °C for 12 h and at 750 °C for 16 h, respectively. The bilayer of YBCO-NCO ceramic was formed by a hot-pressing method. The YBCO powder was first loaded into the graphite mold and the NCO powder was then added on top of the YBCO (see Fig. 1 (a)). After placing a graphite pellet on top of the NCO powder, a graphite plunger was then used to provide a weight of 1 ton and the materials were subjected to the temperature of 800 °C for 1 h under Ar atmosphere.

The phase and crystal structure of each side of the bilayer (Fig. 1 (b)) were analyzed by X-ray diffraction (XRD, Lab X-6000). The grain size was determined by a linear intercept method. The density of the bilayer was calculated using the following equation,

$$\rho_{total} = \rho_{YBCO}V_{YBCO} + \rho_{NCO}V_{NCO} \quad (2)$$

where ρ is the density of each material and V is the volume fraction (i.e. $V_{YBCO} + V_{NCO} = 1$) [11, 12]. Scanning electron microscopy (SEM, JSM-IT300LV) was used for microstructural characterization. Chemical composition measurement was carried out using an energy dispersive spectroscopy (EDS) mode of the SEM instrument.

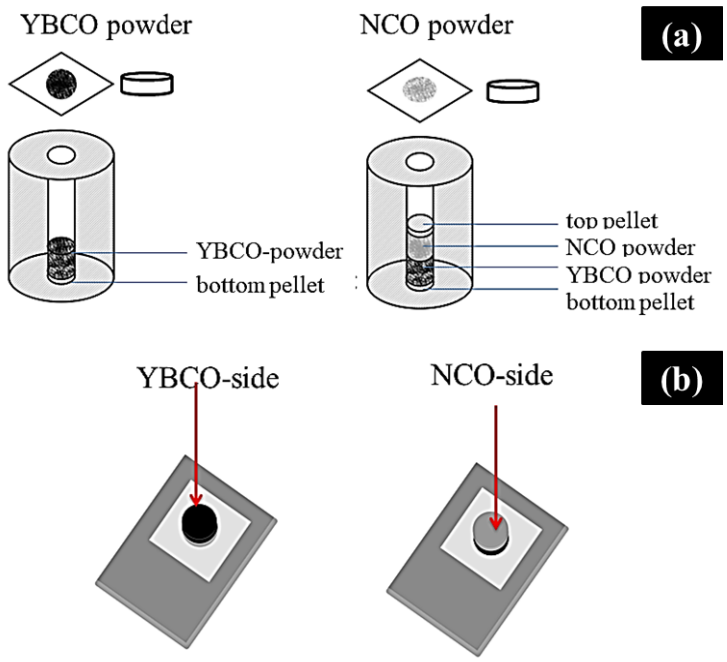

Fig. 1 Schematic drawings showing (a) the process of loading YBCO and NCO powders into a mold and (b) YBCO-side and NCO-side during XRD analysis.

3. Results and Discussion

The XRD result of YBCO powder calcined 850 °C for 12 h and NCO calcined 750 °C for 16 h are shown in Fig. 2. It was found that both YBCO and NCO powders showed nearly single phase. The relative intensity and positions of peaks corresponded to the standard powder patterns. Although some small peaks maybe present, their intensities were near the background noise level and were difficult to be identified. The broadening of some peaks likely came from the effect of X-ray wavelength used which was close to the absorption edge of Co element in the sample. The morphology of the YBCO powder showed irregular shape while that of NCO powder showed small-plate morphology (see Fig. 3). The chemical compositions of the YBCO and NCO powders are shown in Table 1.

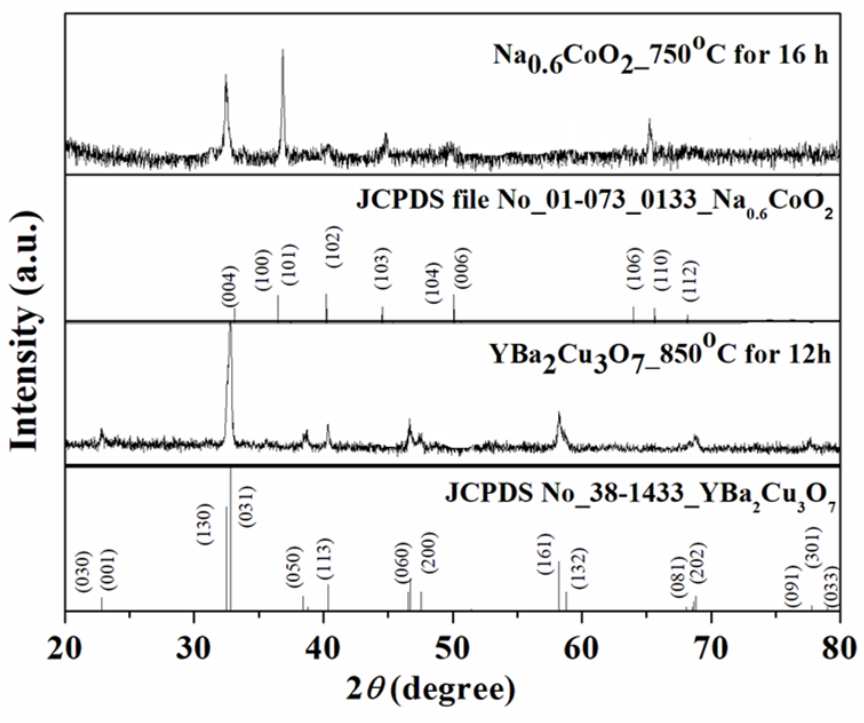

Fig. 2 XRD patterns of (a) YBCO powder and (b) NCO powder.

Table 1 Chemical composition values from EDS analysis of YBCO and NCO powder.

Element	Atomic % EDS	Atomic % Nominal	Weight % EDS	Weight % Nominal
Y	7.93	7.69	14.76	13.35
Ba	13.29	15.38	43.37	41.23
Cu	25.29	23.08	27.56	28.62
O	53.49	53.85	14.31	16.80
Na	15.33	16.67	14.04	13.41
Co	28.16	27.78	52.28	56.12
O	56.51	55.55	33.68	30.47

The EDS results of the calcined YBCO and NCO powders indicated the compositions which were in agreement with the nominal compositions (i.e. $YBa_2Cu_3O_7$ and $Na_{0.6}CoO_2$) used during synthesis. This also helped confirm the phases present as analyzed by X-ray diffraction. The irregular shape and agglomeration of the calcined powders seemed to be the typical feature for both compounds regardless of the synthesis method used [13]. The approximated particle sizes for YBCO and NCO were ≤1 μm and 1 – 10 μm, respectively.

The XRD patterns at room temperature of each side of the segmented YBCO-NCO ceramic are shown in Fig. 4. The XRD pattern of the YBCO-side could be compared with the JCPDS file number 38-1433 of YBa_2CuO_7 which was similar to that reported by Prayoonphokkharat *et al.* [7] and Wannasut *et al.* [10]. The NCO-side could be matched with JCPDS file number 01-073-0133 of $Na_{0.6}CoO_2$ which was also in agreement with the result obtained by Boontham *et al.* [9]. In addition, the XRD patterns of these ceramics were not different from their original calcined powders except a small variation of XRD peak intensities due to the difference in grain size and orientation compared

to the powder cases. Based on these results, the joining of these two structurally and chemically different compounds did not cause any extensive reaction or decomposition of the individual compounds.

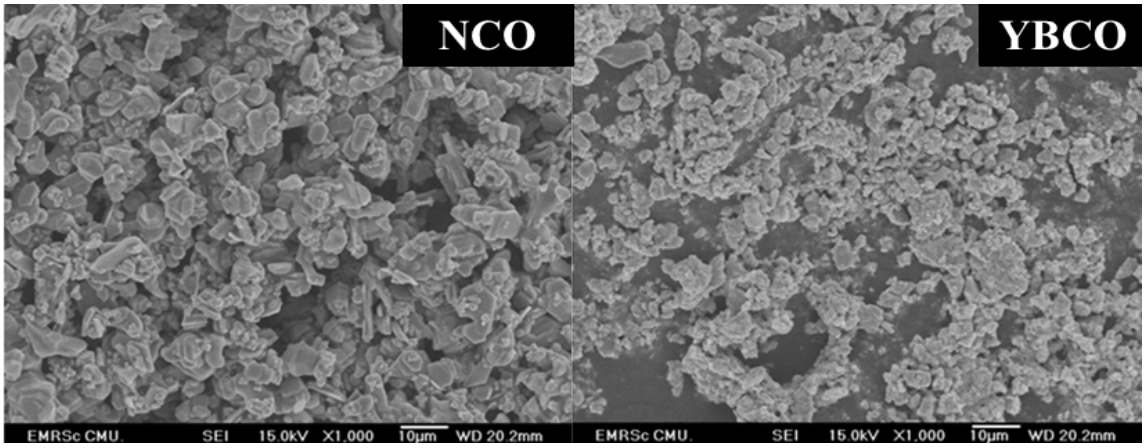

Fig. 3 SEM image of YBCO powder calcined at 850 °C for 12 h and NCO powder calcined at 750 °C for 1 h.

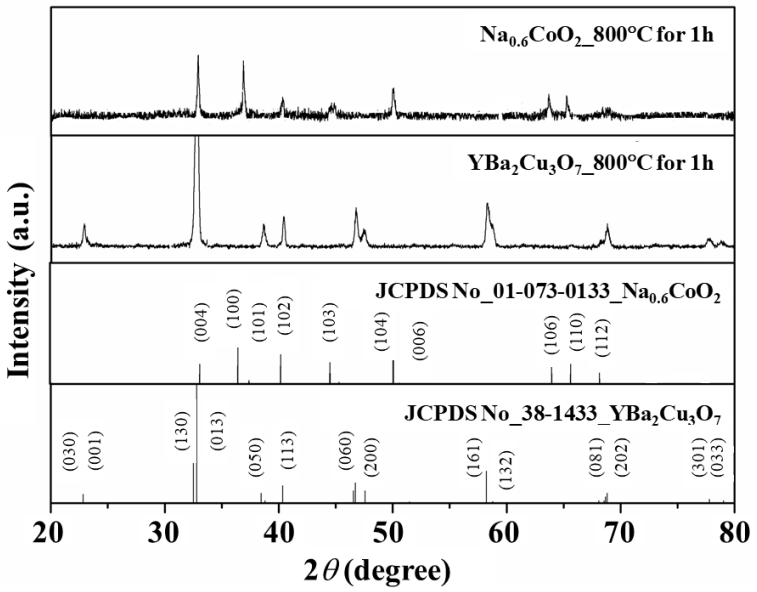

Fig. 4 XRD patterns of each side of the bilayer YBCO-NCO ceramic**.**

The physical properties measurements of the bi-layer sample showed a linear shrinkage of about 18% with high relative density (~97% of theoretical value). SEM backscattered image of the segmented YBCO-NCO ceramic is shown in Fig. 5. A sharp interface could be observed between two compounds. The chemical compositions at various positions (see Fig. 5) are presented in Table 2.

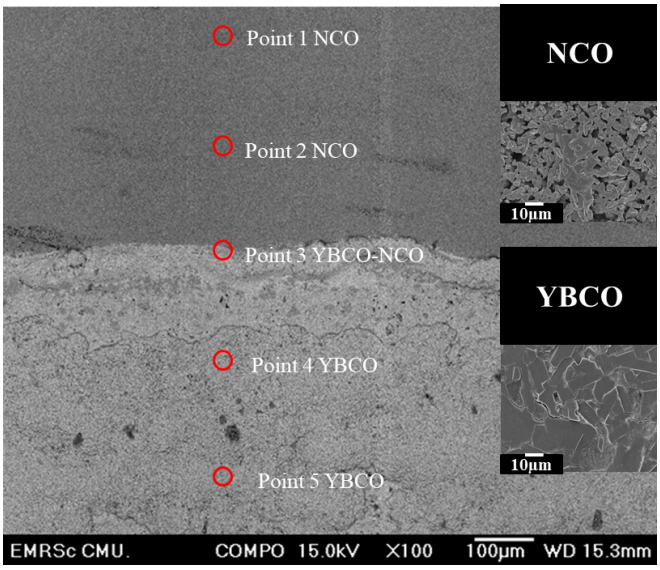

Fig. 5 SEM back-scattered image of bilayer YBCO-NCO ceramic.

The interface of the bilayer presented good bonding with a sharp boundary between YBCO and NCO layer. Based on the SEM image, it was clear that the bilayer was consisted of two homogeneous phases on each side. YBCO-side featured anisotropic shaped grains with the average grain length ~5.22 – 37.31 µm and width ~2.80 – 17.20 µm (approximated from the as-sintered surface which is not shown here). NCO-side presented irregular-shaped grains with the average grain size of ~5.20 µm**.** YBCO showed lighter color compared with NCO. This difference in color was due to the sensitivity of BSE electrons to the average atomic number of each compound [14], i.e. higher average atomic number would give lighter-colored image.

The EDS scan at several points across the bi-layer boundary was performed and the results are shown in Table 2. At the interface, all elements were detected which may be due to the interaction volume of the electron beam that covered both the YBCO and NCO side. In addition, inter-boundary diffusion of some elements was expected which could act as a source of strong chemical bonding. About several hundred micrometers away from the interface, no element diffusing across the boundary was observed. However, the concentration of some elements (e.g. Y in the YBCO side and Na in the NCO side) seemed to be deviated from the expected stoichiometry. Since the hot-pressing procedure was carried out under Ar atmosphere, some elemental defects such as oxygen vacancies may be present which could induce some ionic diffusion within each layer during the sintering process. Since the thickness of each layer was ~2 mm, this region was considered very narrow. It was believed that the overall average composition of each layer should correspond to the stoichiometric composition which was confirmed by the XRD analysis on the surface of YBCO and NCO layers.

Detailed investigation at the interface is now being carried out in order to confirm the inter-layer diffusion as well as any reaction that might occur. Moreover, the sample in this work showed high density (i.e. 4.97 g cm^{-3} or of the theoretical value) despite the relatively low temperature and small-time duration used. Therefore, the hot-pressing procedure seemed to be an effective method to produce bilayer and multilayer oxide thermoelectric ceramics for module production.

Table 2 chemical composition values from EDS analysis of segmented YBCO-NCO.

Spectrum (atomic %)	Y	Ba	Cu	Na	Co	O
point 1 NCO	-	-	-	23.92	29.92	46.15
point 2 NCO	-	-	-	24.17	24.79	51.04
point 3 YBCO-NCO	3.27	5.69	9.51	22.52	10.44	48.57
point 4 YBCO	6.52	12.66	17.81	-	-	63.01
point 5 YBCO	12.73	16.17	16.81	-	-	54.29

4. Conclusion

In this work, the bilayer YBCO-NCO ceramics was successfully prepared by hot- pressing methods using the sintering condition of 800°C for 1 h and the pressure of 1 ton. The ceramics show a high relative density of 97% and good bonding without cracking. The phase and composition of YBCO and NCO layers remained virtually the same despite being sintered under reducing atmosphere. The result indicated that the hot-pressing method can be used to produce high-quality segmented ceramic with less processing time and lower temperature.

5. Acknowledgements

This research was financially supported by the Thailand Research Fund (TRF-RSA5880005 and IRG5780013) and Thailand Institute of Scientific and Technological Research. Partial supports from the Center of Excellence in Materials Science and Materials Technology, the National Research University Project under Thailand's Office of the Higher Education. Faculty of Science, and the Graduate School, Chiang Mai University are also acknowledged. We would also like to thank Center of Excellence in Alternative Energy, Sakon Nakhon Rajabhat University for the hot-press equipment. P. Wannasut would also like to thank the financial support from the TRF through the Royal Golden Jubilee Ph.D Program (PhD 0173/2558).

6. References

[1] Q.H. Wang, J.Z. Zhang, L.L. Zhang, Z.S. Wang, Heat to electricity conversion efficiency measurement for thermoelectric unicouple, KEM. 336 (2007) 883 – 887.

[2] A. Dawongsa, W. Detkunthong, W. Somkhunthot, Fabrication of thermoelectric generator using local minerals at Loei Province, Thailand, SNRUJST. 8(1) (2016) 204 – 210.

[3] T. Caillat, J.P. Fleurial, J. Snyder, A. Zoltan, D. Zoltan, A. Borshchevsky, A new high efficiency segmented thermoelectric, 34th Intersociety Energy Conversion Engineering Conference, Vancouver, British Columbia. 2 – 5 August 1999, 2567 – 2570.

[4] P.H. Ngan, D.V. Christensen, G.J. Snyder, L.T. Hung, S. Linderoth, N.V. Nong, N. Pryds, Towards high efficiency segmented thermoelectric unicouples, Phys. Status. Solid. A. 211(1) (2014) 9 – 17.

[5] X. Wei, R.S. Nagarajan, E. Peng, J. Xue, J. Wang, Fabrication of $YBa_2Cu_3O_{7-x}$ (YBCO) superconductor bulk structures by extrusion free forming, Ceram. Int. 42(14) (2016) 15836 – 15842.

[6] J.M. Tarascon, W.R. Mckinnon, L.H. Greene, G.W. Hull, E.M. Vogel, Oxygen and rare-earth doping of the 90-K superconducting perovskite $YBa_2Cu_3O_{7-x}$, Phys. Rev. B. 36 (1987) 226 – 234.

[7] P. Prayoonphokkharat, A.Watcharapasorn, Transport properties and thermoelectric figure of merit of $YBa_2Cu_3O_{7-x}$–$Bi_{0.5}Na_{0.5}TiO_3$ ceramics, Sci. Adv. Mater. 8 (2016) 1 – 4.

[8] J.E. Rodriguez, J. Lopez, Thermoelectric figure of merit of oxygen-deficient YBCO perovskites, Physica B. 387 (2007) 143 – 146.

[9] S. Boontham, S. Jiansirisomboon, A. Watcharapasorn, Effects of $Bi_{0.5}Na_{0.5}TiO_3$ dopant on microstructure and thermoelectric properties of Na_xCoO_2 ceramics, Nano. Sci. Nanotecno. 15 (2015) 1 – 4.

[10] P. Wannasut, N. Keawprak, A. Watcharapasorn, Preparation of Bilayer $YBa_2Cu_3O_{7-x}$-$NayCoO_2$, Thermoelectric ceramic by solid-state sintering method, Chiang Mai J. Sci. 45(3) (2018) 1 – 6.

[11] P. Jaiban, S. Jiansirisomboon, A. Watcharapasorn, Densification of $Bi_{0.5}Na_{0.5}ZrO_3$ ceramic using liquid-phase sintering method, Science Asia. 37 (2011) 256 – 261.

[12] P. Jaita, Effects of Bismuth Sodium Titanate and Doped Bismuth Sodium Titanate Additions on Structure and Properties of Lead Zirconate Titanate Ceramics, Master Thesis in Materials Science, Chiang Mai University, Chiang Mai, 2009.

[13] N.K. Samin, R. Rusdi, N. Kamarudin, N. Kamarulzaman, Synthesis and battery studies of sodium cobalt oxides, $NaCoO_2$ cathodes, AMR. 545 (2012) 185 – 189.

[14] I.G. Joseph, E.N. Dale, E. Patrick, C.J. David, A.D. Jr. Roming, F. Charles, L. Eric, Scanning Electron Microscopy and X-ray Microanalysis, A Text for Biologists, Materials Scientists, and Geologists, secound ed., Plenum press, New York, 1992.